SUPPORTING INFORMATION

Fe-N-Doped Carbon Capsules with Outstanding Electrochemical Performance and Stability for the Oxygen Reduction Reaction in Both Acid and Alkaline Conditions

Guillermo A. Ferrero, Kathrin Preuss, Adam Marinovic, Ana Belen Jorge, Noramalina Mansor, Dan J. L. Brett, Antonio B. Fuertes, Marta Sevilla,* Maria-Magdalena Titirici*

Table S1. Summary of reported ORR performance for heteroatom-doped carbon catalysts in alkaline media (0.1 M KOH).

Sample	Mass loading (mg cm^{-2})	Onset Potential (V *vs.* RHE)	Kinetic current density (mA cm^{-2})	Ref.
Fe-N-CC	0.10	0.94	18.3 (@ 0.58 V)	This work
NMCS-3	0.66	~ 0.86	-	1
NHPCM-1000	0.32	0.88	6.19 (@ 0.6 V)	2
NZ-13	0.21	~ 0.93	-	3
N-Fe-C@CNTs	0.09	0.88	-	4
N-OMCS-1.5-900	1.00	0.77	-	5
Meso/micro-PoPD	0.50	~ 0.90	-	6
Meso-EmG	0.81	1 V	-	7
***m*-NC-600**	1.14	0.92	10.54 (@ 0.57)	8
NC-A	0.128	0.90	33.24 (@ 0.34 V)	9
N-MCN	0.40	~ 0.83	-	10
SNGL-20	0.306	~ 0.88	10 (@ 0.73 V)	11
N-doped mesoporous nanosheets	0.60	0.97	-	12
N-doped carbon spheres	0.25	0.88	-	13
N-doped graphene	0.05	~ 0.95	~ 6.7 (@ 0.58 V)	14
R/Fe (~0.05 %)	0.21	~ 0.90	-	15
BP-NFe	0.40	1.06	-	16
PANI-4.5Fe-T2(SBA-15)		0.95	7.4 (@ 0.82 V)	17
N-Fe-co-doped CNTs	0.485	0.93	-	18
Fe-N-CNFs	0.60	0.93	48.15 (@ 0.53 V)	19
Fe-N/C	0.10	0.92	-	20
Fe–N–C–700	0.03	0.93	19.4 (@ 0.58 V)	21
Fe–N–C–900	0.03	~ 0.90	10.3 (@ 0.58 V)	21
Fe3C@NCNF-900	0.15	~0.98	~ 15 (@ 0.4 V)	22

Table S2. Summary of reported ORR performance for heteroatom-doped carbon catalysts in acidic media.

Sample	Electrolyte	Mass loading (mg cm^{-2})	Onset Potential (V *vs.* RHE)	Kinetic current density (mA cm^{-2})	Ref.
Fe-N-CC	0.5 M H_2SO_4	0.10	0.80	4.85 (@ 0.46 V)	This work
NZ-13	0.05 M H_2SO_4	0.21	~ 0.81	-	3
Meso/micro-PoPD	Unknown	0.50	0.84	-	6
N-doped mesoporous nanosheets	0.5 M H_2SO_4	0.60	0.75	-	12
N-doped Carbon Spheres	0.5 M H_2SO_4	0.25	0.65	-	13
N-doped graphene	0.5 M H_2SO_4	0.05	~ 0.76	0.5 (@ 0.47 V)	14
N-Fe-co-doped CNTs	0.1 M $HClO_4$	0.49	0.89	-	18
Fe-N-CNFs	0.5 M H_2SO_4	0.60	0.79	-	19
Fe-N/C	0.1 M $HClO_4$	0.10	~ 0.78	-	20
Fe–N–C–700	0.5 M H_2SO_4	0.03	0.89	-	21
Fe–N–C–900	0.5 M H_2SO_4	0.03	0.85	-	21
Fe-N-HCMS	0.5 M H_2SO_4	0.25	0.80	4.6 (@ 0.6 V)	23
Fe3C@NCNF-900	0.1 M $HClO_4$	0.15	0.78	-	22

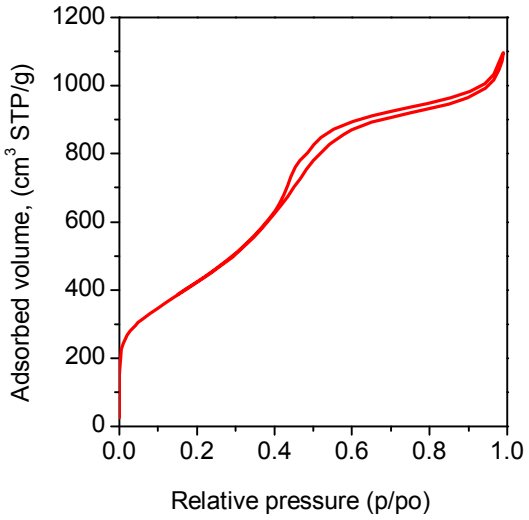

Figure S1. Nitrogen sorption isotherm of the Fe-N-doped carbon capsules (Fe-N-CC).

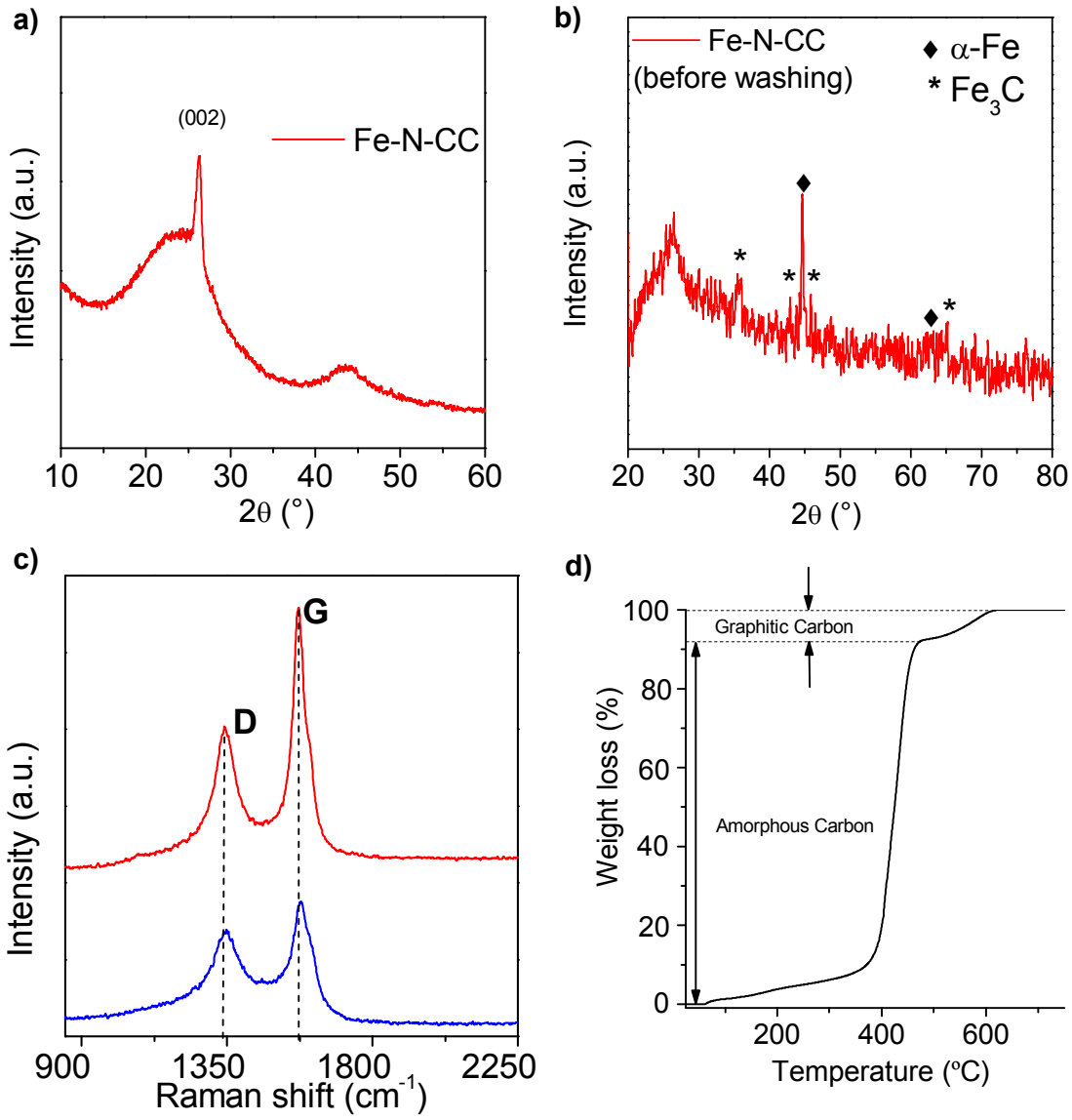

Figure S2. XRD pattern of the Fe-N-CC (a) after and (b) before washing, (c) Raman spectra of amorphous (blue line) and graphitic carbon regions (red line), and (d) TGA analysis of Fe-N-CC in air.

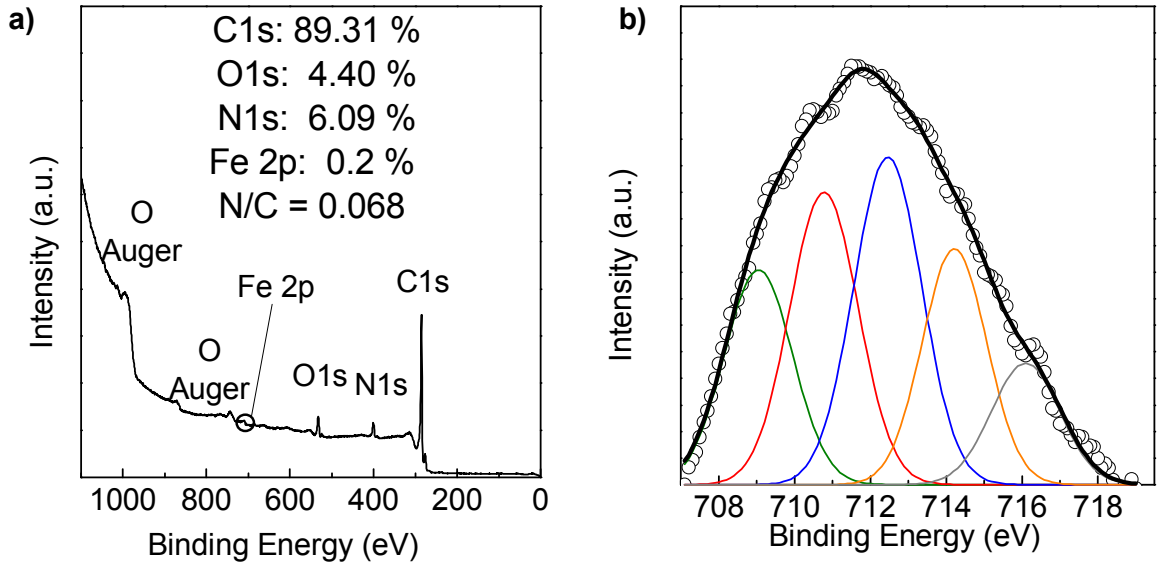

Figure S3. (a) XPS general spectrum of Fe-N-CC and (b) high-resolution Fe $2p_{3/2}$ XPS spectrum.

As can be seen in Figure S3b, the Fe $2p_{3/2}$ XPS spectra shows multiple peaks, which indicates that metal species in the catalysts are complicated in terms of their chemical state. According to previous reports, the Fe $2p_{3/2}$ peak located at around 712 eV is due to N-coordinated iron.[19, 24] This metal species and Fe_3C have been demonstrated to be the main responsible active centers on iron and nitrogen co-doped carbon materials.[25, 26] However, no peak corresponding to Fe_3C (located at 706.7-706.9 eV)[27, 28] can be identified, which agrees with the TEM/HRTEM studies that show its encapsulation in a relatively thick graphitic carbon layer. The other peaks may be attributed to Fe^{2+} (709.05 eV) and Fe^{3+} (710.8 eV), and the corresponding satellite peaks (714.3 and 716.1 eV respectively). [29, 30] As shown by previous studies, these peaks may as well correspond to N-coordinated iron.[20, 31]

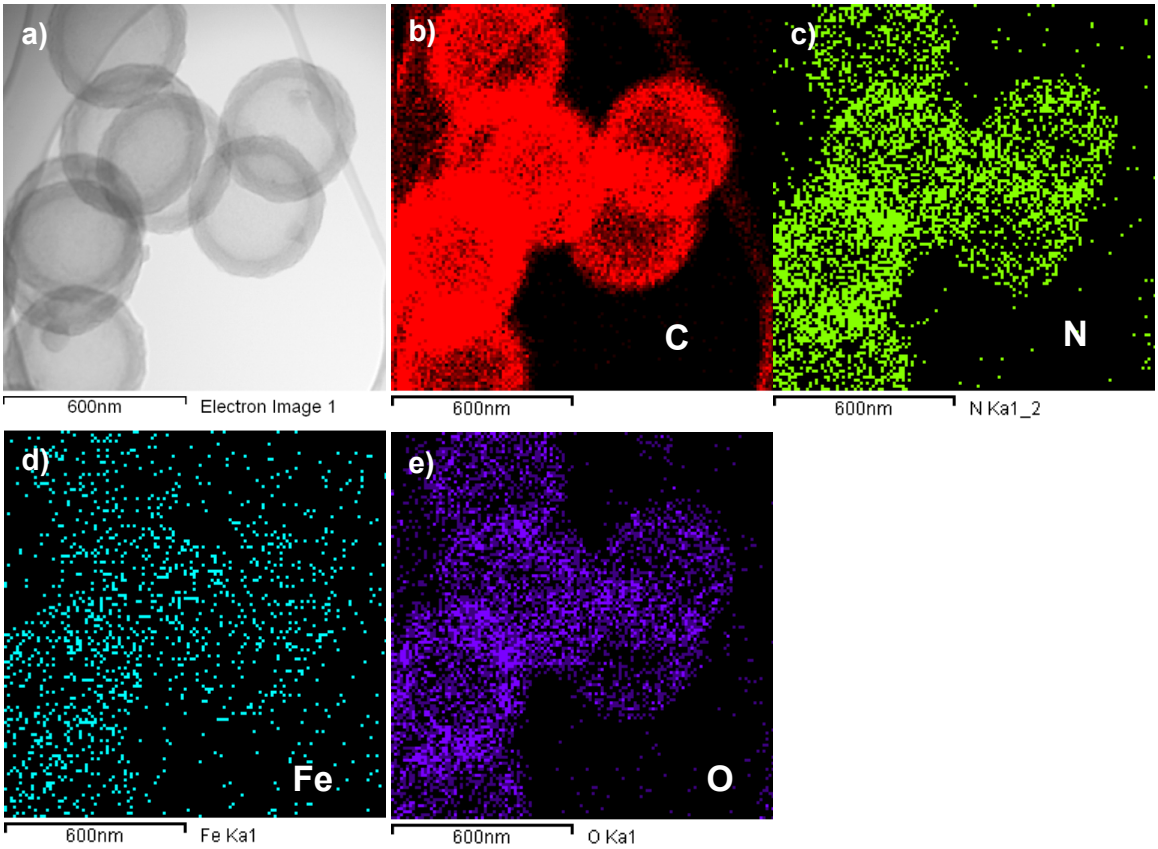

Figure S4. (a) TEM image and its corresponding EDX mappings for (b) carbon, (c) nitrogen, (d) iron and (e) oxygen for the corresponding Fe-N-CC.

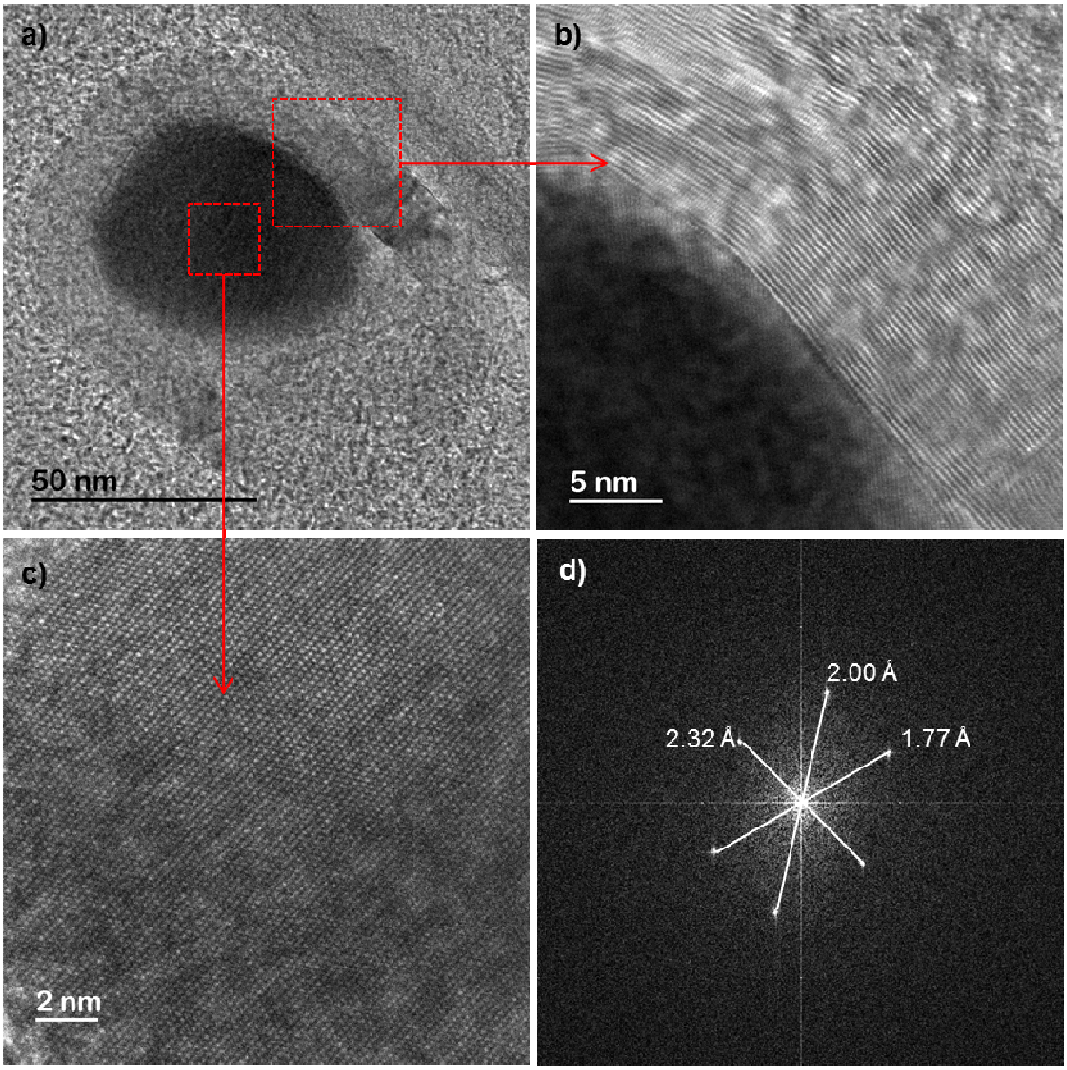

Figure S5. (a) HRTEM image of a Fe_3C nanoparticle, (b) an enlarged HRTEM image of the graphitic layer, (c) an enlarged HRTEM image of the Fe_3C nanoparticle and (d) its SAED pattern.

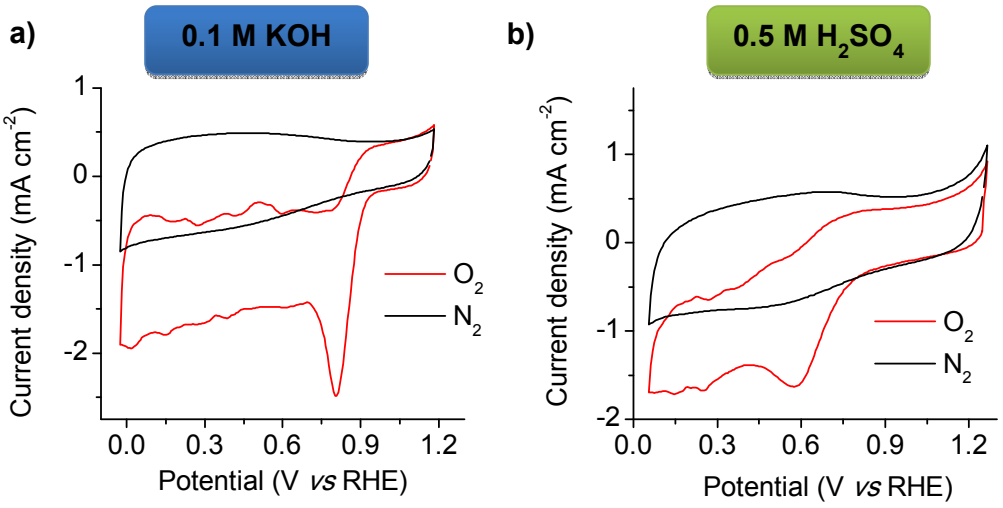

Figure S6. Cyclic voltammograms of Fe-N-CC in N_2 and O_2 saturated (a) 0.1 M KOH and (b) 0.5 M H_2SO_4 electrolytes.

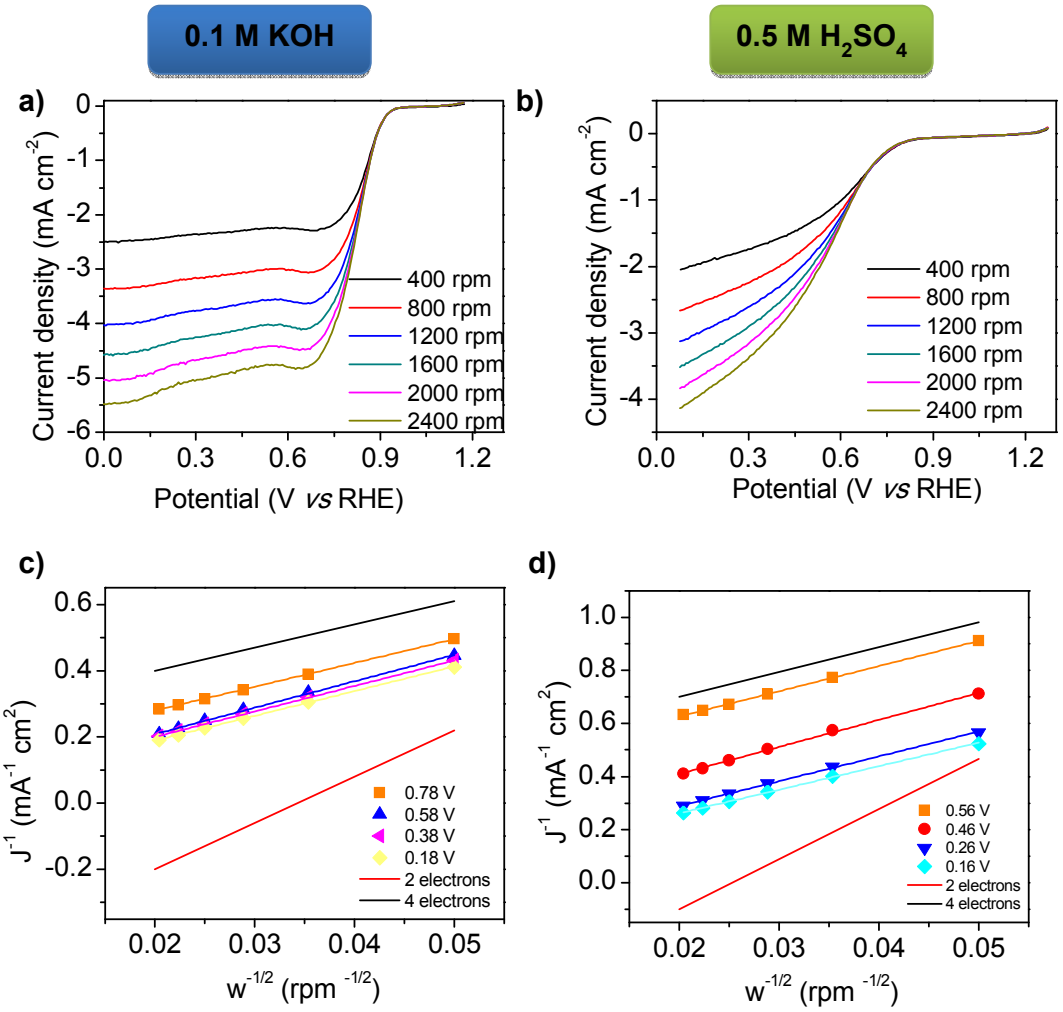

Figure S7. LSVs at 10 mV s^{-1} in the presence of oxygen with rotation speed from 400 to 2400 rpm in (a) 0.1 M KOH and (b) 0.5 M H_2SO_4, and the corresponding Koutecky-Levich plots in (c) 0.1 M KOH and (d) 0.1 M H_2SO_4, compared with those of an ideal 2-electron process (red line) and an ideal 4-electron process (black line).

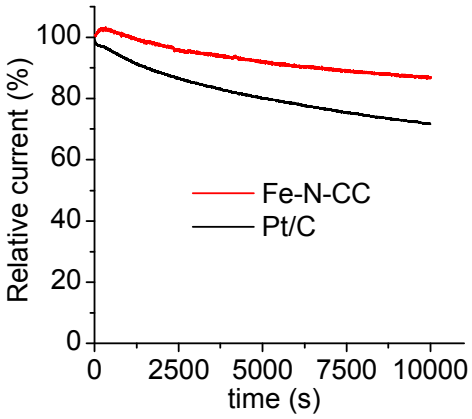

Figure S8. Comparison of the chronoamperometric response of Fe-N-CC and Pt/C over 10,000 s at 0.68 V and a constant rotation speed of 800 rpm in O_2-saturated solution 0.1 M KOH.

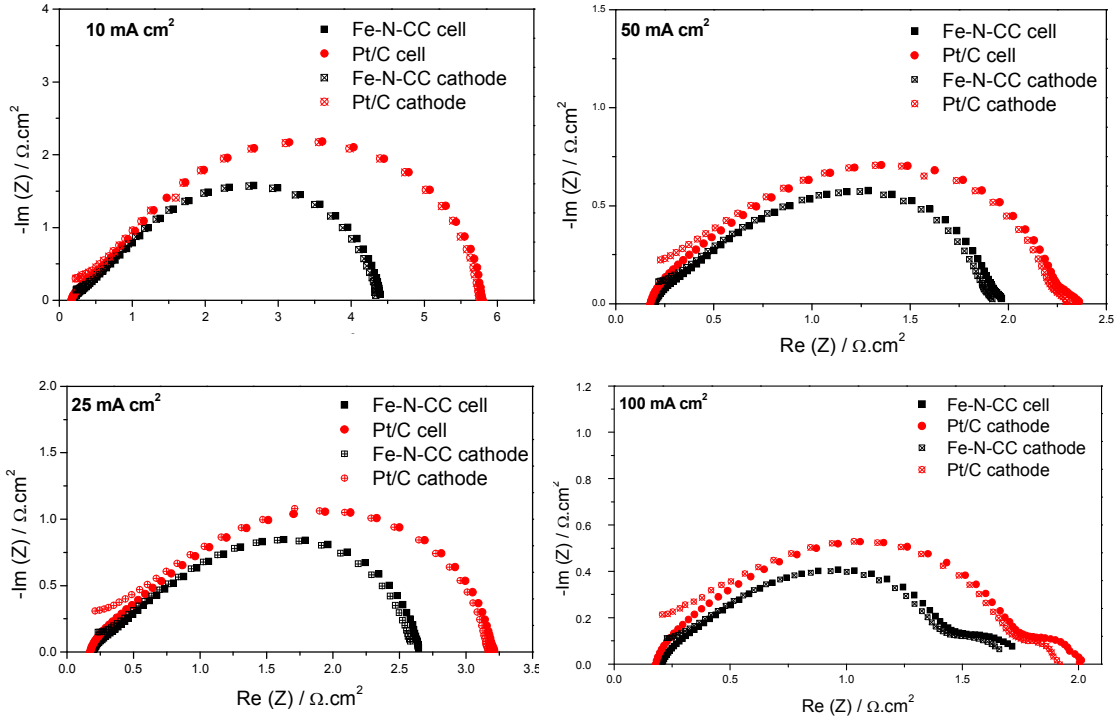

Figure S9. Nyquist plots of the whole cell, including the half-cell measurements of the cathode, at current densities in the 10 – 100 mA cm^{-2} range. Anode half-cell measurements are not shown for clarity.

References

1. Tang, J.; Liu, J.; Li, C.; Li, Y.; Tade, M. O.; Dai, S.; Yamauchi, Y. Synthesis of Nitrogen-Doped Mesoporous Carbon Spheres with Extra-Large Pores through Assembly of Diblock Copolymer Micelles. *Angew. Chem. Int. Ed.* **2015**, 54, 588-593.
2. Chen, Y.; Ma, R.; Zhou, Z.; Liu, G.; Zhou, Y.; Liu, Q.; Kaskel, S.; Wang, J. An In Situ Source-Template-Interface Reaction Route to 3D Nitrogen-Doped Hierarchical Porous Carbon as Oxygen Reduction Electrocatalyst. *Adv. Mater. Interfaces* **2015**, 2.
3. Elumeeva, K.; Fechler, N.; Fellinger, T. P.; Antonietti, M. Metal-Free Ionic Liquid-Derived Electrocatalyst for High-Performance Oxygen Reduction in Acidic and Alkaline Electrolytes. *Mater. Horiz.* **2014**, 1, 588-594.
4. Hu, C.; Wang, L.; Zhao, Y.; Ye, M.; Chen, Q.; Feng, Z.; Qu, L. Designing Nitrogen-Enriched Echinus-Like Carbon Capsules for Highly Efficient Oxygen Reduction Reaction and Lithium Ion Storage. *Nanoscale* **2014**, 6, 8002-8009.
5. Li, J.; Li, Z.; Tong, J.; Xia, C.; Li, F. Nitrogen-Doped Ordered Mesoporous Carbon Sphere with Short Channel as an Efficient Metal-Free Catalyst for Oxygen Reduction Reaction. *RSC Adv.* **2015**, 5, 70010-70016.
6. Liang, H.-W.; Zhuang, X.; Brüller, S.; Feng, X.; Müllen, K. Hierarchically Porous Carbons with Optimized Nitrogen Doping as Highly Active Electrocatalysts for Oxygen Reduction. *Nat. Commun.* **2014**, 5.
7. Yang, W.; Fellinger, T.-P.; Antonietti, M. Efficient Metal-Free Oxygen Reduction in Alkaline Medium on High-Surface-Area Mesoporous Nitrogen-Doped Carbons Made from Ionic Liquids and Nucleobases. *J. Am. Chem. Soc.* **2011**, 133, 206-209.
8. Liu, X.; Zhu, H.; Yang, X. One-step Synthesis of Dopamine-Derived Micro/Mesoporous Nitrogen-Doped Carbon Materials for Highly Efficient Oxygen-Reduction Catalysts. *J. Power Sources* **2014**, 262, 414-420.
9. He, W.; Jiang, C.; Wang, J.; Lu, L. High-Rate Oxygen Electroreduction over Graphitic-N Species Exposed on 3D Hierarchically Porous Nitrogen-Doped Carbons. *Angew. Chem. Int. Ed.* **2014**, 53, 9503-9507.
10. Yang, T.; Liu, J.; Zhou, R.; Chen, Z.; Xu, H.; Qiao, S. Z.; Monteiro, M. J. N-Doped Mesoporous Carbon Spheres as the Oxygen Reduction Reaction Catalysts. *J. Mater. Chem. A* **2014**, 2, 18139-18146.
11. Xu, J.; Dong, G.; Jin, C.; Huang, M.; Guan, L. Sulfur and Nitrogen Co-Doped, Few-Layered Graphene Oxide as a Highly Efficient Electrocatalyst for the Oxygen-Reduction Reaction. *ChemSusChem* **2013**, 6, 493-499.
12. Wei, W.; Liang, H.; Parvez, K.; Zhuang, X.; Feng, X.; Müllen, K. Nitrogen-Doped Carbon Nanosheets with Size-Defined Mesopores as Highly Efficient Metal-Free Catalyst for the Oxygen Reduction Reaction. *Angew. Chem. Int. Ed.* **2014**, 53, 1570-1574.
13. Ai, K.; Liu, Y.; Ruan, C.; Lu, L.; Lu, G. Sp^2 C-Dominant N-Doped Carbon Sub-micrometer Spheres with a Tunable Size: A Versatile Platform for Highly Efficient Oxygen-Reduction Catalysts. *Adv. Mater.* **2013**, 25, 998-1003.
14. Parvez, K.; Yang, S.; Hernandez, Y.; Winter, A.; Turchanin, A.; Feng, X.; Müllen, K. Nitrogen-Doped Graphene and Its Iron-Based Composite As Efficient

Electrocatalysts for Oxygen Reduction Reaction. *ACS Nano* **2012**, 6, 9541-9550.
15. Masa, J.; Zhao, A.; Xia, W.; Sun, Z.; Mei, B.; Muhler, M.; Schuhmann, W. Trace Metal Residues Promote the Activity of Supposedly Metal-Free Nitrogen-Modified Carbon Catalysts for the Oxygen Reduction Reaction. *Electrochem. Commun.* **2013**, 34, 113-116.
16. Liu, J.; Sun, X.; Song, P.; Zhang, Y.; Xing, W.; Xu, W. High-Performance Oxygen Reduction Electrocatalysts Based on Cheap Carbon Black, Nitrogen, and Trace Iron. *Adv. Mater.* **2013**, 25, 6879-6883.
17. Yan, X.-H.; Xu, B.-Q. Mesoporous Carbon Material Co-Doped with Nitrogen and Iron (Fe-N-C): High-Performance Cathode Catalyst for Oxygen Reduction Reaction in Alkaline Electrolyte. *J. Mater. Chem. A* **2014**, 2, 8617-8622.
18. Li, Y.; Zhou, W.; Wang, H.; Xie, L.; Liang, Y.; Wei, F.; Idrobo, J.-C.; Pennycook, S. J.; Dai, H. An Oxygen Reduction Electrocatalyst Based on Carbon Nanotube-Graphene Complexes. *Nat. Nano* **2012**, 7, 394-400.
19. Wu, Z.-Y.; Xu, X.-X.; Hu, B.-C.; Liang, H.-W.; Lin, Y.; Chen, L.-F.; Yu, S.-H. Iron Carbide Nanoparticles Encapsulated in Mesoporous Fe-N-Doped Carbon Nanofibers for Efficient Electrocatalysis. *Angew. Chem. Int. Ed.* **2015**, 54, 8179-8183.
20. Lin, L.; Zhu, Q.; Xu, A.-W. Noble-Metal-Free Fe–N/C Catalyst for Highly Efficient Oxygen Reduction Reaction under Both Alkaline and Acidic Conditions. *J. Am. Chem. Soc.* **2014**, 136, 11027-11033.
21. Kong, A.; Dong, B.; Zhu, X.; Kong, Y.; Zhang, J.; Shan, Y. Ordered Mesoporous Fe-Porphyrin-Like Architectures as Excellent Cathode Materials for the Oxygen Reduction Reaction in Both Alkaline and Acidic Media. *Chem. Eur. J.* **2013**, 19, 16170-16175.
22. Ren, G.; Lu, X.; Li, Y.; Zhu, Y.; Dai, L.; Jiang, L. Porous Core–Shell Fe3C Embedded N-doped Carbon Nanofibers as an Effective Electrocatalysts for Oxygen Reduction Reaction. *ACS Appl. Mater. Interfaces* **2016**, 8, 4118-4125.
23. Zhou, M.; Yang, C.; Chan, K.-Y. Structuring Porous Iron-Nitrogen-Doped Carbon in a Core/Shell Geometry for the Oxygen Reduction Reaction. *Adv. Energy Mater.* **2014**, 4.
24. Zhao, Y.; Watanabe, K.; Hashimoto, K. Self-Supporting Oxygen Reduction Electrocatalysts Made from a Nitrogen-Rich Network Polymer. *J. Am. Chem. Soc.* **2012**, 134, 19528-19531.
25. Tylus, U.; Jia, Q.; Strickland, K.; Ramaswamy, N.; Serov, A.; Atanassov, P.; Mukerjee, S. Elucidating Oxygen Reduction Active Sites in Pyrolyzed Metal–Nitrogen Coordinated Non-Precious-Metal Electrocatalyst Systems. *J. Phys. Chem. C* **2014**, 118, 8999-9008.
26. Wei, J.; Liang, Y.; Hu, Y.; Kong, B.; Simon, G. P.; Zhang, J.; Jiang, S. P.; Wang, H. A Versatile Iron–Tannin-Framework Ink Coating Strategy to Fabricate Biomass-Derived Iron Carbide/Fe-N-Carbon Catalysts for Efficient Oxygen Reduction. *Angew. Chem. Int. Ed.* **2016**, 55, 1355-1359.
27. Wu, G.; Chen, Z.; Artyushkova, K.; Garzon, F. H.; Zelenay, P. Polyaniline-Derived Non-Precious Catalyst for the Polymer Electrolyte Fuel Cell Cathode. *Ecs Transactions* **2008**, 16, 159-170.
28. Maldonado, S.; Stevenson, K. J. Direct Preparation of Carbon Nanofiber Electrodes via Pyrolysis of Iron(II) Phthalocyanine: Electrocatalytic Aspects for Oxygen Reduction. *J. Phys. Chem. B* **2004**, 108, 11375-11383.

29. Devaux, R.; Vouagner, D.; de Becdelievre, A. M.; Duret-Thual, C. Electrochemical and Surface Studies of the Ageing of Passive Layers Grown on Stainless Steel in Neutral Chloride Solution. *Corros. Sci.* **1994**, 36, 171-186.
30. Yang, W.; Costa, D.; Marcus, P. Resistance to Pitting and Chemical Composition of Passive Films of a Fe-17% Cr Alloy in Chloride-Containing Acid Solution. *J. Electrochem. Soc.* **1994**, 141, 2669-2676.
31. Niu, W.; Li, L.; Liu, X.; Wang, N.; Liu, J.; Zhou, W.; Tang, Z.; Chen, S. Mesoporous N-Doped Carbons Prepared with Thermally Removable Nanoparticle Templates: An Efficient Electrocatalyst for Oxygen Reduction Reaction. *J. Am. Chem. Soc.* **2015**, 137, 5555-5562.